

1 Conference Proceedings Paper

2 Mathematical tools that connect different indexing 3 analyses

4 Ryoko Oishi-Tomiyasu^{1,*}

5 ¹ Institute of Mathematics for Industry, Kyushu University; tomiyasu@imi.kyushu-u.ac.jp

6 * Correspondence: tomiyasu@imi.kyushu-u.ac.jp;

7 Received: date; Accepted: date; Published: date

8 **Abstract:** As mathematical tools that can be commonly used for indexing analyses from different
9 types of experimental patterns, we have recently developed (i) rules on forbidden *hkl*'s that can be
10 used even when the space group and setting are unknown, (ii) algorithm for error-stable Bravais
11 lattice determination, (iii) generalization of the de Wolff figure of merit for powder diffraction (1D
12 data) to data in higher-dimensions such as Kikuchi patterns (2D data) by electron backscatter
13 diffraction (EBSD). In particular, (ii) could be used in a variety of situations, not just for indexing. It
14 is explained how (i)–(iii) are used in the mathematical framework of our indexing algorithms. The
15 developed software is now available on the web.

16 Powder auto-indexing: <https://z-code.kek.jp/zrg/> (CONOGRAPH)

17 EBSD ab-initio indexing: <https://osdn.net/projects/ebbsd-conograph/>

18 **Keywords:** Bravais lattice; ab-initio indexing; figure of merit

20 1. Introduction

21 Mathematical tools that can be commonly used in ab-initio indexing analyses are introduced
22 herein. They were originally invented for powder diffraction [1], and subsequently applied to
23 indexing of Kikuchi bands in electron backscatter diffraction (EBSD) patterns [2]. “Ab-initio” means
24 that the indexing is carried out without any prior information on the parameters and Bravais type of
25 the unit cell.

26 In the case of powder diffraction, the values of *d*-spacings (hence, lengths of reciprocal-lattice
27 vectors) are obtained from positions of diffraction peaks. In the EBSD case, the orientations of
28 reciprocal-lattice vectors are provided from the positions of Kikuchi bands. Our indexing algorithms
29 for them use a common mathematical framework shown in Figure 1. First, the parameters of the
30 primitive cell are determined, because (i) simple rules of systematic absence are available, if only
31 basis vectors of a primitive lattice are considered. Subsequently, (ii) Bravais-type (and centering)
32 determination is carried out. This process can be error-stable enough to deal with unit-cell parameters
33 containing large errors due to zero-point shifts (powder [3]) or projection-center shifts (EBSD [4]). We
34 also (iii) generalized the idea of the de Wolff figure of merit M_r [5], which has been the most efficient
35 indicator in powder indexing. The generalized one presents similar properties for EBSD patterns [2].

36 In what follows, the mathematics used for (ii) is mainly discussed. Due to the limitation of the
37 space, (i), (iii) are only mentioned, referring to published papers. The author believes that these
38 theoretical results will be also useful in different analyses of crystallography.

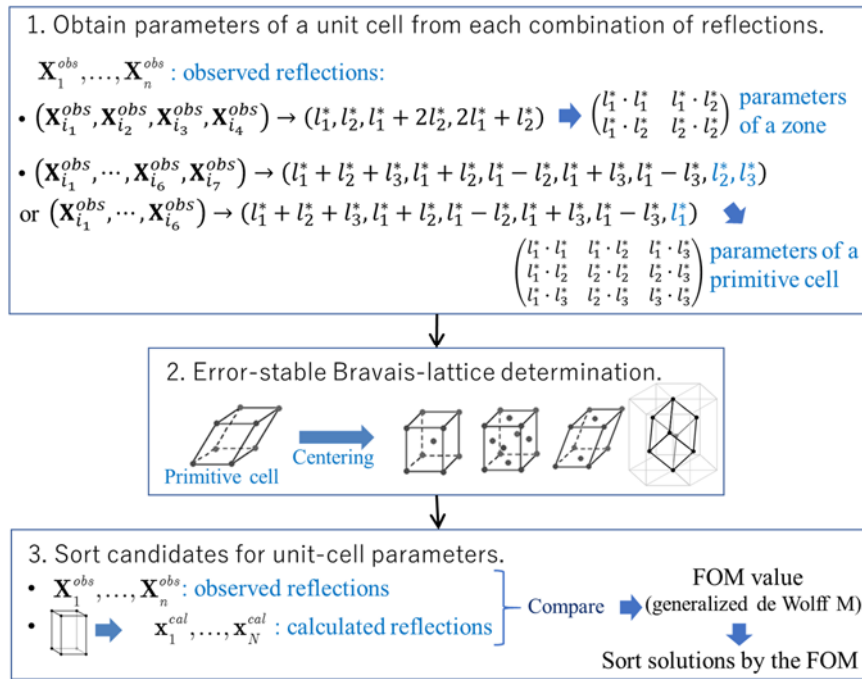


Figure 1. Common mathematical framework of our indexing algorithms

39 1.1. Notation

40 We summarize the notation and symbols used in the article. The inner product of the Euclidean
 41 space \mathbb{R}^N is denoted by $u \cdot v$, and the Euclidean norm $u \cdot u$ is denoted by $|u|^2$. Any basis
 42 v_1, \dots, v_N of an N -dimensional(N -D) lattice L is associated to a quadratic form:

$$f(x_1, \dots, x_N) = |x_1 v_1 + \dots + x_N v_N|^2 = \mathbf{x}^T S \mathbf{x}, \quad (1)$$

43 where $\mathbf{x} = (x_1, \dots, x_N)^T$ is a vector, and S is the symmetric matrix with $v_i \cdot v_j$ in the
 44 (i, j) -entry. S is also the Gramian (or metric tensor [6]) of L . The stabilizer of S is defined as the
 45 following subgroup of $GL_N(\mathbb{Z})$ (= the group of integral matrices with the determinant ± 1):

$$\text{Stab}(S) = \{g \in GL_N(\mathbb{Z}) : gSg^T = S\}. \quad (2)$$

46 The Gramians S_1, S_2 belong to the same Bravais type, if $\text{Stab}(S_1), \text{Stab}(S_2)$ are conjugate in
 47 $GL_N(\mathbb{Z})$ (i.e., there exists $\sigma \in GL_N(\mathbb{Z})$ such that $\sigma \text{Stab}(S_1) \sigma^{-1} = \text{Stab}(S_2)$) [7].

48 On the linear space \mathcal{S}_N consisting of N -by- N symmetric matrices, an inner product is defined
 49 by $S \bullet T := \text{Trace}(ST)$, which makes \mathcal{S}_N the metric space (the distance between S and T equals
 50 $(S - T) \bullet (S - T)$). The subset of \mathcal{S}_N consisting of all the positive definite symmetric matrices is
 51 denoted by \mathcal{S}_N^+ . The action of $GL_N(\mathbb{Z})$ on \mathcal{S}_N^+ is given by $S \mapsto gSg^T$.

52 The following is an overview of the lattice-basis reduction theory that discusses methods to
 53 provide the representatives for the orbits $GL_N(\mathbb{Z}) \backslash \mathcal{S}_N^+$. Namely, $\mathcal{D} \subset \mathcal{S}_N^+$ is the subset that
 54 fulfills the following (i), (ii):

55 (i) $\mathcal{S}_N^+ = \bigcup_{g \in GL_N(\mathbb{Z})} \mathcal{D}[g],$

56 (ii) $\mathcal{D}[g_1] \cap \mathcal{D}[g_2] = \emptyset$ for any $g_1 \neq \pm g_2 \in GL_N(\mathbb{Z})$, where $\mathcal{D}[g] \stackrel{def}{=} \{gSg^T : S \in \mathcal{D}\}.$

57 As the boundaries of \mathcal{D} are prone to complications, overlaps of the boundary
 58 $\partial\mathcal{D} := \mathcal{D} \setminus \mathcal{D}^{in}$ (\mathcal{D}^{in} : set of interior points of \mathcal{D}) are frequently allowed. In such a case, \mathcal{D}
 59 should satisfies (i) and the following (ii)' and (iii)':

60 (ii)' $\mathcal{D}^{in}[g_1] \cap \mathcal{D}^{in}[g_2] = \emptyset$ for any $g_1 \neq \pm g_2 \in GL_N(\mathbb{Z})$.

61 (iii)' $\mathcal{D} \cap \mathcal{D}[g] \neq \emptyset$ for only finitely many $g \in GL_N(\mathbb{Z})$.

62 It is straightforward to see that any S in \mathcal{D}^{in} satisfies $\text{Stab}(S) = \{\pm 1\}$. Thus, all the S
 63 with non-triclinic Bravais types belong to the boundary of \mathcal{D} . The following are the definitions of
 64 Venkov [8] and Delaunay reductions used in Section 3; for any fixed $S_0 \in \mathcal{S}_N^+$, define \mathcal{D}_{S_0} by:

$$\mathcal{D}_{S_0} := \{S \in \mathcal{S}_N^+ : S \bullet S_0 \leq (gSg^T) \bullet S_0 \text{ for any } g \in GL_N(\mathbb{Z})\}. \quad (3)$$

65 From the definition, $\mathcal{D}_{S_0}[g] = \mathcal{D}_{S_0} \Leftrightarrow g^T \in \text{Stab}(S_0)$ holds. If S belongs to \mathcal{D}_{S_0} , S is
 66 Venkov-reduced with regard to S_0 . In particular, S is Selling-reduced, if S belongs to \mathcal{D}_{A_N} , where A_N
 67 is the symmetric matrix with 2 in the diagonal entries and 1 in the other entries.

$$A_N(i, j) = \begin{cases} 2 & i = j, \\ 1 & i \neq j. \end{cases} \quad (4)$$

68

69 **2. Determination of the primitive lattice**

70 For some types of SA, forbidden reflections are not exceptional, but occur considerably high rate.
 71 The rules of SA stated in International Tables depend on the space group and setting of atomic
 72 positions. Simpler rules of SA are required for developing algorithms that generally work.

73 In order to obtain such simple rules, only basis vectors of the primitive lattice are considered
 74 herein. L^* is the reciprocal lattice of the crystal lattice L . $\{l_1^*, l_2^*\}$ is a primitive set, if it is a subset of
 75 some basis l_1^*, l_2^*, l_3^* of L^* .

76

77 **Theorem 1.** [Theorem 2, [9]] *Regardless of the type of SA, there are infinitely many primitive sets $\{l_1^*, l_2^*\}$*
 78 *of L^* such that none of $l_1^*, l_2^*, l_1^* + 2l_2^*, 2l_1^* + l_2^*$ corresponds to an extinct reflection due to the SA.*
 79 *Furthermore, there exist infinitely many 2D sublattices L_2^* of L^* such that L_2^* is expanded by such l_1^*, l_2^* .*

80

81 Theorem1 is not true, if $l_1^*, l_2^*, l_1^* + 2l_2^*, 2l_1^* + l_2^*$ are replaced e.g., by $l_1^*, l_2^*, l_1^* + l_2^*, l_1^* - l_2^*$

82 (vectors in Ito's formula[10]: $2\left(\left|l_1^*\right|^2 + \left|l_2^*\right|^2\right) = \left|l_1^* + l_2^*\right|^2 + \left|l_1^* - l_2^*\right|^2$). The theorem assures that some

83 combinations of observed reflections correspond to $l_1^*, l_2^*, l_1^* + 2l_2^*, 2l_1^* + l_2^*$, for some l_1^*, l_2^* contained

84 in a basis of L^* . In the powder case, the inner product $l_1^* \cdot l_2^*$ is computed by

$$l_1^* \cdot l_2^* = \left(|l_1^* + 2l_2^*|^2 - |l_1^*|^2 - 4|l_2^*|^2 \right) / 4 = \left(|2l_1^* + l_2^*|^2 - 4|l_1^*|^2 - |l_2^*|^2 \right) / 4. \quad (5)$$

85 Similarly, in the EBSD case, the direction $l^*/|l^*|$ of the reciprocal-lattice vector l are obtained from
 86 the coordinates of Kikuchi bands. Therefore, the vector-length ratio $|l_1^*| : |l_2^*| : |l_1^* + 2l_2^*|$ can be
 87 calculated from the directions of $l_1^*/|l_1^*|, l_2^*/|l_2^*|, (l_1^* + 2l_2^*)/|l_1^* + 2l_2^*|$ by solving the linear equation.

$$\begin{pmatrix} l_1^*/|l_1^*| & 2l_2^*/|l_2^*| & -(l_1^* + 2l_2^*)/|l_1^* + 2l_2^*| \end{pmatrix} \mathbf{x} = 0 \quad (6)$$

88 In both of Eq.(5), (6), the lengths (or directions) of $l_1^*, l_2^*, l_1^* + 2l_2^*$ are sufficient to obtain the
 89 matrix (or the ratio of its components) in Eq.(7). The remaining length (or direction) of $2l_1^* + l_2^*$ can
 90 be used to remove unlikely solutions quickly.

$$\begin{pmatrix} l_1^* \cdot l_1^* & l_1^* \cdot l_2^* \\ l_1^* \cdot l_2^* & l_2^* \cdot l_2^* \end{pmatrix} \quad (7)$$

91 Theorem 2 is a 3D version of Theorem 1.

92

93 **Theorem 2.** [Theorem 4 in [9]] *Regardless of the type of SA, there are infinitely many bases $\langle l_1^*, l_2^*, l_3^* \rangle$ of*
 94 *L^* such that the following hold:*

95 (a) *the reflections of $\pm l_1^* + l_2^* + l_3^*$ are not forbidden.*

96 (b) *For both $i = 2, 3$, (i) none of the reflections of $ml_1^* + (m-1)(-l_1^* + l_i^*)$ are forbidden for any*
 97 *integer m , or (ii) none of the reflections of $ml_i^* + (m-1)(l_1^* - l_i^*)$ are forbidden for any integer*
 98 *$m \geq 0$.*

99

100 As a result, in CONOGRAPH, $l_1^* \pm l_2^*, l_1^* \pm l_3^*, l_1^* + l_2^* + l_3^*$ and either of l_1^* or $\{l_2^*, l_3^*\}$ are
 101 assigned to various combinations of observed reflections. See Figure 5 of [2] for the EBSD case.

102

103 3. Bravais-lattice determination from unit-cell parameters containing large observation errors

104 3.1. theoretical Background

105 After the parameters of the primitive cell are obtained in the indexing process, it is necessary to
 106 convert them into parameters of the conventional cell. For a Gramian matrix S^{obs} extracted from
 107 observed data, how can one estimate the Bravais type of the unknown true value \hat{S} of S^{obs} ? In
 108 practice, the error can be observational errors or rounding errors of floating-point numbers [11].

109 If S^{obs} is exact (i.e., $S^{obs} = \hat{S}$), the symmetry group of n -by- n S^{obs} can be determined e.g., by
 110 the method of [12] (the computation time is rapidly augmented as n increases). However, if $S^{obs} \neq \hat{S}$,
 111 no matter how close S^{obs} is to \hat{S} , $g \in \text{Stab}(S^{obs})$ is not generally true for any $1 \neq g \in \text{Stab}(\hat{S})$.

112 As a result, it is only possible to estimate likely ones as $\text{Stab}(\hat{S})$. It is common in libraries developed
 113 by mathematicians (e.g., *Magma* [13]) that the parameters of a lattice cannot be entered in floating-type
 114 numbers. For this reason, error-stable methods have been investigated in mathematical crystallography.

115 This determination can be done by step 1 & 2 in Table 1 by using a finite set H_0 with the following
 116 property, where \mathcal{D} is a domain that fulfills (i), (ii)', (iii)' in Section 1.1.
 117

118 H_0 : if $S^{obs} \in \mathcal{D}$, then $\hat{S} \in \cup_{g \in H_0} \mathcal{D}[g]$.

119 Namely, H_0 is a finite set containing all $g \in GL_N(\mathbb{Z})$ such that $g^{-1}S^{obs}(g^{-1})^T$ is nearly
 120 reduced (i.e., close to \mathcal{D}) for some reduced S^{obs} (i.e., S^{obs} that belongs to \mathcal{D}).
 121

122 **Table 1. Outline of error-stable Bravais lattice determination methods¹**

Prepared sets in codes	1. For a domain \mathcal{D} that fulfills (i), (ii)', (iii)' in Section 1.1, and its topological closure $\overline{\mathcal{D}}$, let G_0 be the finite set consisting of all $g \in GL_N(\mathbb{Z})$ with $\overline{\mathcal{D}} \cap \overline{\mathcal{D}[g]} \neq \emptyset$. For each finite group G_k ($k = 1, \dots, m$) contained in G_0 , prepare the set of linear subspace L_k consisting of all $S \in \mathcal{S}_n$ with $\text{Stab}(S) \supset G_k$. (Namely, L_1, \dots, L_m are <i>lattice characters</i> [6].) 2. Finite set H_0 consisting of operations g for which $\mathcal{D}[g]$ may contain \hat{S} when S^{obs} is in \mathcal{D} .
Input parameters	Gramian S^{obs} (assume $S^{obs} \in \mathcal{D}$ by exchanging the basis)
Step 1	For any $g \in H_0$, if $S_2^{obs} = g^{-1}S^{obs}(g^{-1})^T$ is close to the domain $\overline{\mathcal{D}}$ within the error of S^{obs} (i.e., nearly reduced), do the following; for each L_k ($k = 1, \dots, m$), calculate $S \in L_k$ close to S_2^{obs} e.g., by projecting S_2^{obs} on L_k . If S_2^{obs} and S are close to each other within the error, store g, S in the array for the Bravais type of L_k .
Step 2	Output the stored g, S after removing duplicates.

123 ¹ The same calculation can be done, even if \mathcal{D} is replaced by a union of finitely many $\mathcal{D}[g]$ such as the
 124 Venkov reduced domain \mathcal{D}_{S_0} . The only difference is that L_k may not be in the boundary of $\overline{\mathcal{D}}$.

125 If \mathcal{D} is the Niggli-reduced domain [Chap.9.2.2, 6], G_0 in Table 1 consists of 168 elements. The
 126 number m of lattice characters L_k is 42, after two triclinic cases are excluded [Table 9.2.5.1, 6]. H_0 must
 127 contain G_0 , because all the non-triclinic S belong to the boundary of the Niggli-reduced domain. Hence,
 128 the computation time of the method of Table 1 is roughly estimated as $|H_0| \times m \geq 168 \times 42 = 7056$. This is
 129 a little time consuming, if it is applied to multiple primitive cells generated in the indexing process.

130 The methods of Andrews & Bernstein [14,15] are basically same as this Niggli-reduced case,
 131 although it is not assured that their heuristics can always generate all the necessary operations (in their
 132 method, 25 operations in [16] are used to generate the elements of H_0).

133 Use of the Delaunay reduced domain was proposed Burzlaff & Zimmermann [17,18]. This reduces
 134 the number of lattice characters from 44 to 30. However, H_0 is set to $\{ 1 \}$ in their method, so it can
 135 basically handle only the exact case.

136 Thus, the following are the problems, in order to develop a faster and more reliable Bravais-lattice
 137 determination method.
 138

139 **Question 1:** Which reduction method minimizes the computation time for Table 1?

140 **Question 2:** Under which assumption on the error size of S^{obs} , is it possible to output all the S with
 141 $S^{obs} \approx S$ and $\text{Stab}(S) = \text{Stab}(\hat{S})$?

142

143 Our idea for **Question 1** was to use the following Venkov-reduced domain \mathcal{D}_{S_0} as \mathcal{D} in Table 1.

144 • $S_0 = I_3$ (3×3 identity matrix): if \mathcal{D} is the Niggli-reduced domain,

$$\mathcal{D}_{I_3} = \bigcup_{g \in \text{Stab}(I_3)} \mathcal{D}[g^T] \tag{8}$$

145 • $S_0 = A_3$ in Eq.(4): if \mathcal{D} is the Delaunay-reduced domain,

$$\mathcal{D}_{A_3} = \bigcup_{g \in \text{Stab}(A_3)} \mathcal{D}[g^T] \tag{9}$$

146 By the choice of S_0 , \mathcal{D}_{S_0} can include non-triclinic L_k in the interior distant from its boundary $\partial\mathcal{D}_{S_0}$.

147 In such a case, if \hat{S} is in L_k and Venkov-reduced with regard to S_0 , $S^{obs} \approx \hat{S}$ is also in the interior of

148 \mathcal{D}_{S_0} . As a result, it is not necessary to consider the nearly-reduced. H_0 may be set to $\{1\}$ if the Venkov

149 reduction is used.

150 Based on this idea, the author proved that error-stable determination is possible, under the
 151 following condition C on the error size of S^{obs} [19] (This is an answer to **Question 2**):

152

153 C : for any 3-by-3 symmetric matrix T and $0 \neq \mathbf{v} \in \mathbb{Z}^n$, if $\hat{S} \bullet T \geq \mathbf{v} \hat{S} \mathbf{v}^T / 2$, $S^{obs} \bullet T > 0$ holds.

154

155 Namely, C excludes the case: $\mathbf{v}^T S \mathbf{v} / 2 \leq \hat{S} \bullet T \approx S^{obs} \bullet T \leq 0$ (If L is the crystal lattice with

156 the Gramian \hat{S} , the half of the squared-length of any non-zero vector in L is observed as a positive

157 value). Hence, C only assumes that the error of S^{obs} is not extraordinary large. Under this condition,

158 the following is proved:

159 **Theorem 3.** [Theorem 1--4 in [19]] For a given $S^{obs} \in \mathcal{D}_{S_0}$, assume that \hat{S} belongs to the Bravais

160 type B , in addition to C . In this case, \hat{S} belongs to the V_B , a union of finitely many linear subspaces
 161 in Table 2.

162

163

Table 2. B, S_0, V_B in Theorem 1.

Bravais type B	S_0	$H_0 = \{1\}$?	The number of linear subspaces V_B (the number when $H_0 = \{1\}$ holds)
Primitive monoclinic	I_3	Yes	3 (3) ... Table 3 in [19]
Face-centered orthorhombic	A_3	Yes	3 (3) ... Table 4 in [19]
Body-centered orthorhombic ¹	A_3	Yes	... Table 5 in [19]
Rhombohedral	A_3	conditionally yes ²	64 (16) ... Table 6 in [19]
Base-centered monoclinic	A_3	conditionally yes ²	69 (21) ... Table 8 in [19]

164 ¹ As for the face-centered case, our method simply uses the fact that S^{obs} has the face-centered symmetry if
 165 and only if the inverse of S^{obs} has the body-centered symmetry.

166 ² This is yes, if the software user only needs the S closest to S^{obs} among those with the Bravais type B .

167

168 There are only 5 Bravais types in Table 2, because it is straightforward to classify unit cells after
169 the centering determination (i.e., conventional unit cells) into higher-symmetric Bravais types.

170 In Table 2, if $H_0 = \{1\}$, the number of operations required for the error-stable determination is same
171 as the exact case. Therefore, contrary to our intuition, it is possible to output S with $S^{obs} \approx S$ and
172 $\text{Stab}(S) = \text{Stab}(\hat{S})$ very generally, without increasing the computation time at all. However, the
173 error of S^{obs} affects the distance between the output S and its true value \hat{S} .

174 3.1. Computation results

175 The implemented program is used in our indexing software [1,2]. It was also used to build a
176 database of quadratic forms [20]. In [2], indexing analysis was carried out for EBSD patterns with
177 projection-centers shifted as follows (z : the camera length).

$$\frac{\Delta x}{z}, \frac{\Delta y}{z}, \frac{\Delta z}{z} = 0, \pm 0.005, \pm 0.01, \pm 0.02 \quad (10)$$

178 The software succeeded in indexing of orthorhombic–cubic cells in most of the cases. Among
179 them, there were only a few failures due to errors in Bravais-lattice determination (see Tables 4,5 and
180 Figure 9 in [2] for more details).

181 5. Discussion

182 The theorems presented in Sections 2, 3 hold true for any symmetry types the crystal structures
183 can have. Our error-stable Bravais-type determination is probably the first method where the result
184 is mathematically guaranteed, even for parameters with large error. As I explained, the number of
185 operations $|H_0| \times m \geq 168 \times 42 = 7056$ cannot be decreased as long as the Niggli reduction is used, although
186 it can be reduced from 7056 to 154 (58, conditionally) by using the Venkov reduction for I_3 and A_3 .
187 However, there might be other reduction methods (or S_0) that provide a faster method. No studies have
188 been reported for lattices of dimensions more than 3.

189 Prior to such theoretical results, software developers of indexing analysis had to develop case-
190 by-case algorithms or heuristics to deal with the symmetries by themselves. As ab-initio indexing
191 software for powder diffraction patterns, *ITO* [21,22], *TREOR* [23], and *DICVOL* [24] are well known.
192 EBSD ab-initio indexing have been also studied in [25–27], although more accurate methods for band
193 extraction and projection center identification are also needed for this indexing analysis.

194 From a theoretical point of view, the two indexing analyses have much in common. This
195 suggests that updating the mathematical crystallography is effective to obtain reliable and efficient
196 analytical methods in short time.

197 **Funding:** This study was financially supported by the PREST (JPMJPR14E6) and JST Mirai (JPMJMI18GD)

198 **Acknowledgments:** We would like to extend our gratitude to Mr. R. Taniguchi and Mr. S. E. Graiff-Zurita of
199 Kyushu University, who helped us in coding the software, and performing the computation.

200 **Conflicts of Interest:** The authors declare no conflict of interest.

201 References

- 202 1. Oishi-Tomiyasu, R. Robust powder auto-indexing using many peaks. *J. Appl. Cryst.*, **2014**, *47*, 593–598.
203 doi.org/10.1107/S1600576714000922
- 204 2. Oishi-Tomiyasu, R., Tanaka, T., Nakagawa, J. Distribution rules of systematic absence and generalized de
205 Wolff figure of merit applied to EBSD ab-initio indexing. <https://arxiv.org/abs/2003.13403>.
- 206 3. Dong, C.; Wu, F.; Chen, H. Correction of zero shift in powder diffraction patterns using the reflection-pair
207 method. *J. Appl. Cryst.* **1999**, *32*, 850–853. [doi:10.1107/S0021889899007396](https://doi.org/10.1107/S0021889899007396)

- 208 4. Ram, F.; Zaefferer, S.; Jäpel, T.; Raabe, D. Error analysis of the crystal orientations and disorientations
209 obtained by the classical electron backscatter diffraction technique. *J. Appl. Cryst.*, **2015**, *48*, 797–813.
210 [doi:10.1107/S1600576715005762](https://doi.org/10.1107/S1600576715005762)
- 211 5. de Wolff, P. M. A Simplified Criterion for the Reliability of a Powder Pattern Indexing. *J. Appl. Cryst.* **1968**,
212 *1*, 108–113. [doi:10.1107/S002188986800508X](https://doi.org/10.1107/S002188986800508X)
- 213 6. Hahn, T. *et.al.* International Tables for Crystallography Vol.A, 5th ed.; Publisher: Springer, **2005**.
- 214 7. Michel, L. Symmetry, invariants, topology. iv. fundamental concepts for the study of crystal symmetry.
215 *Physics Reports*, **2001**, *341*, 265–336.
- 216 8. Venkov, B. A. On the reduction of positive quadratic forms. *Izv. Akad. Nauk SSSR Ser. Mat.*, **1940**, *134*, 37–
217 52.
- 218 9. Oishi-Tomiyasu, R. Distribution rules of systematic absences on the Conway topograph and their
219 application to powder auto-indexing. *Acta Cryst.*, **2013**, *A69*, 603–610. [doi:10.1107/S0108767313021740](https://doi.org/10.1107/S0108767313021740)
- 220 10. Ito, T. A general powder X-ray photography. *Nature*, **1949**, *164*, 755–756. [doi:10.1038/164755a0](https://doi.org/10.1038/164755a0)
- 221 11. Grosse-Kunstleve, R. W.; Sauter, N. K.; Adams, P. D. Numerically stable algorithms for the computation of
222 reduced unit cells. *Acta Cryst.*, **2004**, *A60*, 1–6. [doi:10.1107/S010876730302186X](https://doi.org/10.1107/S010876730302186X)
- 223 12. Plesken, W.; Souvignier, B. B. Computing isometries of lattices. *J. Symbolic. Comput.*, **1997**, *24*, 327–334.
224 [doi:10.1006/jsc.1996.0130](https://doi.org/10.1006/jsc.1996.0130)
- 225 13. Bosma, W.; Cannon, J.; Playoust, C. The Magma algebra system. I: The user language. *J. Symbolic Comput.*,
226 **1997**, *24* (3–4), 235–265. [doi:10.1006/jsc.1996.0125](https://doi.org/10.1006/jsc.1996.0125)
- 227 14. Andrews, L. C.; Bernstein, H. J. Lattices and reduced cells as points in 6-space and selection of bravais
228 lattice type by projections. *Acta Cryst.*, **1988**, *A44*, 1009–1018. [doi:10.1107/S0108767388006427](https://doi.org/10.1107/S0108767388006427)
- 229 15. Andrews, L.C.; Bernstein, H. J. The geometry of Niggli reduction: BGAOL--embedding Niggli reduction
230 and analysis of boundaries. *J. Appl. Cryst.* **2014**, *47*(1), 346–359. [doi:10.1107/S1600576714014460](https://doi.org/10.1107/S1600576714014460)
- 231 16. Gruber, B. The relationship between reduced cells in a general Bravais lattice. *Acta Cryst.*, **1973**, *A29*, 433–
232 440. [doi:10.1107/S0567739473001063](https://doi.org/10.1107/S0567739473001063)
- 233 17. Burzlaff, H.; Zimmermann, H. On the metrical properties of lattices. *Z. Kristallogr.*, **1985**, *170*, 247–262.
234 [doi:10.1524/zkri.1985.170.14.247](https://doi.org/10.1524/zkri.1985.170.14.247)
- 235 18. Zimmermann H.; Burzlaff, H. Delos--a computer program for the determination of a unique conventional
236 cell. *Z. Kristallogr.*, **1985**, *170*, 241–246. [doi:10.1524/zkri.1985.170.14.241](https://doi.org/10.1524/zkri.1985.170.14.241)
- 237 19. Oishi-Tomiyasu, R. Rapid bravais-lattice determination algorithm for lattice parameters containing large
238 observation errors. *Acta Cryst. A.*, **2012**, *68*, 525–535. [doi:10.1107/S0108767312024579](https://doi.org/10.1107/S0108767312024579)
- 239 20. Oishi-Tomiyasu, R. Positive-definite ternary quadratic forms with the same representations over Z . *Int. J.*
240 *Number Theory*, **2020**, *16*(7), 1493–1534.
- 241 21. de Wolff, P. M. Detection of simultaneous zone relations among powder diffraction lines. *Acta Cryst.*, **1958**,
242 *11*, 664–665. [doi:10.1107/S0365110X58001729](https://doi.org/10.1107/S0365110X58001729)
- 243 22. Visser, J. W. A fully automatic program for finding the unit cell from powder data. *J. Appl. Cryst.*, **1969**, *2*,
244 89–95. [doi:10.1107/S0021889869006649](https://doi.org/10.1107/S0021889869006649)
- 245 23. Kohlbeck, F.; Horl, E.M. Trial and error indexing program for powder patterns of monoclinic substances.
246 *J. Appl. Cryst.*, **1978**, *11*, 60–61. [doi:10.1107/S0021889878012716](https://doi.org/10.1107/S0021889878012716)
- 247 24. Boultif, A.; Louër, D. Powder pattern indexing with the dichotomy method. *J. Appl. Cryst.*, **2004**, *37*, 724–
248 731. [doi:10.1107/S0021889804014876](https://doi.org/10.1107/S0021889804014876)
- 249 25. Dingley, D. J.; Wright, S. I. Determination of crystal phase from an electron backscatter diffraction pattern.
250 *J. Appl. Cryst.*, **2009**, *42*, 234–241. [doi:10.1107/S0021889809001654](https://doi.org/10.1107/S0021889809001654)
- 251 26. Li, L.; Ouyang, S.; Yang, Y.; Han, M. EBSDL: a computer program for determining an unknown Bravais
252 lattice using a single electron backscatter diffraction pattern. *J. Appl. Cryst.*, **2014**, *47*, 1466–1468.
253 [doi:10.1107/S160057671401382X](https://doi.org/10.1107/S160057671401382X)
- 254 27. Li, L.; Han, M. Determining the Bravais lattice using a single electron backscatter diffraction pattern. *J. Appl.*
255 *Cryst.*, **2015**, *48*, 107–115. doi.org/10.1107/S1600576714025989



© 2020 by the authors. Submitted for possible open access publication under the terms and conditions of the Creative Commons Attribution (CC BY) license (<http://creativecommons.org/licenses/by/4.0/>).